

UWThPh-1997-29
HEPHY-PUB 673/97
DESY 97-169
hep-ph/9709252

Production and Decay of Stops and Sbottoms, and Determination of SUSY Parameters*

A. Bartl^{†1}, H. Eberl^{○2}, T. Gajdosik^{★2}, S. Kraml^{‡2},
W. Majerotto^{§2}, W. Porod^{¶1}, A. Sopczak^{♯3}

(1) *Institut für Theoretische Physik, Universität Wien, A-1090 Vienna, Austria*

(2) *Institut für Hochenergiephysik, Österreichische Akademie der Wissenschaften,
A-1050 Vienna, Austria*

(3) *DESY-Zeuthen, D-15738 Zeuthen, Germany*

Abstract

We present numerical predictions for the decay branching ratios of the heavier stop and sbottom mass eigenstates. We estimate the precision to be expected for the determination of the underlying supersymmetry parameters of the stop and sbottom systems.

1 Introduction

The study of pair production of scalar top quarks is particularly interesting because the lighter stop \tilde{t}_1 is expected to be the lightest scalar quark. Left-right mixing plays a rôle only in the sector of the sfermions of the 3rd generation. Therefore, experimental data about stops will give information about the soft-breaking trilinear scalar coupling parameter A_t .

*Contribution to the proceedings of the "ECFA/DESY Study on Physics and Detectors for the Linear Collider", DESY 97-123E, ed. R. Settles

†bartl@Pap.UniVie.ac.at, ○ helmut@hephy.oeaw.ac.at, ★ garfield@hephy.oeaw.ac.at,

‡ kraml@hephy.oeaw.ac.at, § majer@hephy.oeaw.ac.at, ¶ porod@Pap.UniVie.ac.at,

♯ andre.sopczak@cern.ch; http://wwwhephy.oeaw.ac.at/p3w/theory/susy/

At an e^+e^- Linear Collider with center-of-mass energy $\sqrt{s} \geq 500$ GeV it will be possible to produce the higher stop and sbottom mass eigenstates \tilde{t}_2, \tilde{b}_2 . This will allow a detailed study of the properties of stops and sbottoms. The decay pattern of \tilde{t}_2 and \tilde{b}_2 may be rather complicated, because of left-right mixing, and since many decay channels can be open. In this contribution we will study the decays of \tilde{t}_2 and \tilde{b}_2 , and we will present numerical predictions for the important decay branching ratios. We will also give an estimate of the expected precision for the determination of the underlying soft supersymmetry breaking parameters.

The supersymmetric (SUSY) partners of the Standard Model fermions with left and right helicity are the left and right sfermions. In the case of stop and sbottom the left and right states are in general mixed. In the $(\tilde{f}_L, \tilde{f}_R)$ basis the mass matrix is [1, 2]

$$M_{\tilde{f}}^2 = \begin{pmatrix} m_{\tilde{f}_L}^2 & a_f m_f \\ a_f m_f & m_{\tilde{f}_R}^2 \end{pmatrix} \quad (1)$$

with

$$m_{\tilde{f}_L}^2 = M_{\tilde{Q}}^2 + m_Z^2 \cos 2\beta (T_f^3 - e_f \sin^2 \theta_W) + m_f^2, \quad (2)$$

$$m_{\tilde{f}_R}^2 = M_{\tilde{F}'}^2 + e_f m_Z^2 \cos 2\beta \sin^2 \theta_W + m_f^2, \quad (3)$$

$$a_t \equiv A_t - \mu \cot \beta, \quad a_b \equiv A_b - \mu \tan \beta, \quad (4)$$

where e_f and T_f^3 are the charge and the third component of the weak isospin of the sfermion \tilde{f} , $M_{\tilde{F}'} = M_{\tilde{U}}$, $M_{\tilde{D}}$ for $\tilde{f}_R = \tilde{t}_R, \tilde{b}_R$, respectively, and m_f is the mass of the corresponding fermion. From renormalization group equations [3] one expects that due to the Yukawa interactions the soft SUSY breaking masses $M_{\tilde{Q}}$, $M_{\tilde{U}}$, and $M_{\tilde{D}}$ of the 3rd generation sfermions are smaller than those of the 1st and 2nd generation. \tilde{t}_L - \tilde{t}_R mixing is important because of the large top quark mass [1, 4]. For sbottoms left-right mixing can be important if $\tan \beta \gtrsim 10$ [5, 6]. The mass eigenvalues for the sfermions $\tilde{f} = \tilde{t}, \tilde{b}$ are

$$m_{\tilde{f}_{1,2}}^2 = \frac{1}{2} \left(m_{\tilde{f}_L}^2 + m_{\tilde{f}_R}^2 \mp \sqrt{(m_{\tilde{f}_L}^2 - m_{\tilde{f}_R}^2)^2 + 4m_f^2 a_f^2} \right) \quad (5)$$

where \tilde{t}_1 , and \tilde{b}_1 denote the lighter eigenstates. The mixing angles $\theta_{\tilde{f}}$ are given by

$$\cos \theta_{\tilde{f}} = \frac{-a_f m_f}{\sqrt{(m_{\tilde{f}_L}^2 - m_{\tilde{f}_1}^2)^2 + a_f^2 m_f^2}}, \quad \sin \theta_{\tilde{f}} = \frac{m_{\tilde{f}_L}^2 - m_{\tilde{f}_1}^2}{\sqrt{(m_{\tilde{f}_L}^2 - m_{\tilde{f}_1}^2)^2 + a_f^2 m_f^2}}. \quad (6)$$

2 Decays of Stop and Sbottom

The squarks of the third generation can have the weak decays ($i, j = 1, 2; k = 1, \dots, 4$)

$$\tilde{t}_i \rightarrow t \tilde{\chi}_k^0, \quad b \tilde{\chi}_j^+, \quad (7)$$

$$\tilde{b}_i \rightarrow b \tilde{\chi}_k^0, \quad t \tilde{\chi}_j^-. \quad (8)$$

If the strong decays

$$\tilde{t}_i \rightarrow t \tilde{g}, \quad \tilde{b}_i \rightarrow b \tilde{g} \quad (9)$$

are kinematically allowed then they are the dominant decay modes of \tilde{t}_1 and \tilde{b}_1 . Otherwise, the lighter squark mass eigenstates decay mostly according to (7) and (8). If $m_{\tilde{\chi}_1^0} + m_b + m_W < m_{\tilde{t}_1} < m_{\tilde{\chi}_1^0} + m_t$, then the decay $\tilde{t}_1 \rightarrow b W^+ \tilde{\chi}_1^0$ is important [7], otherwise the loop decay $\tilde{t}_1 \rightarrow c \tilde{\chi}_1^0$ can be dominant for $m_{\tilde{t}_1} < m_b + m_{\tilde{\chi}_1^\pm}$. In case of strong left-right mixing the splitting between the two mass eigenstates may be so large that the following additional decay modes are present [6]:

$$\tilde{t}_2 \rightarrow \tilde{t}_1 Z, \quad \tilde{b}_1 W^+, \quad (10)$$

$$\tilde{b}_2 \rightarrow \tilde{b}_1 Z, \quad \tilde{t}_1 W^-, \quad (11)$$

$$\tilde{t}_2 \rightarrow \tilde{t}_1 h^0 (H^0, A^0), \quad \tilde{b}_1 H^+, \quad (12)$$

$$\tilde{b}_2 \rightarrow \tilde{t}_1 h^0 (H^0, A^0), \quad \tilde{t}_1 H^-. \quad (13)$$

The decay of the lighter eigenstates \tilde{t}_1 and \tilde{b}_1 were studied e. g. in [8, 9]. The decay patterns of the heavier squark mass eigenstates can be quite complicated, because all the decay modes of eqs. (7) to (13) can occur. In the following we will study \tilde{t}_2 and \tilde{b}_2 decays in the parameter domain where the decays (10) to (13) are important. Earlier studies are in [6, 8, 9, 10, 11]. We calculate the different decay widths with the formulae of Refs. [6, 7, 8]. We have included radiative corrections to the Higgs masses and the Higgs mixing angle according to [12]. As examples we will plot the branching ratios of \tilde{t}_2 and \tilde{b}_2 decays as a function of the Higgs–higgsino mass parameter μ , for $\tan \beta = 2$ and 30, $A_t = A_b = 600$ GeV, $M_{\tilde{Q}} = 500$ GeV, $M_{\tilde{U}} = 444$ GeV, $M_{\tilde{D}} = 556$ GeV, taking the SU(2) gaugino mass parameter $M = 200$ GeV, and the mass of the pseudoscalar Higgs boson $m_{A^0} = 130$ GeV. For $\tan \beta = 2$ the mass differences between the higher and lower mass eigenstates are $m_{\tilde{t}_2} - m_{\tilde{t}_1} \geq m_Z$ ($m_{\tilde{t}_2} - m_{\tilde{t}_1} \geq m_{A^0}$) for $\mu \leq 770$ GeV ($\mu \leq 520$ GeV), $m_{\tilde{t}_2} - m_{\tilde{b}_1} \geq m_W$ ($m_{\tilde{t}_2} - m_{\tilde{b}_1} \geq m_{H^+}$) for $\mu \leq 263$ GeV ($\mu \leq -759$ GeV), $m_{\tilde{t}_2} - m_{\tilde{b}_2} \geq m_W$ for $\mu \leq -528$ GeV, $m_{\tilde{b}_2} - m_{\tilde{t}_1} \geq m_{H^+}$ for $\mu \leq 216$ GeV, $m_{\tilde{b}_2} - m_{\tilde{t}_1} \geq m_W$ in the whole μ range considered. Furthermore, the mass of the light neutral Higgs boson is in the range $73 \text{ GeV} \leq m_{h^0} \leq 94 \text{ GeV}$, the mass of the charged Higgs boson is $m_{H^+} = 153$ GeV.

We show in Fig. 1a the branching ratios of \tilde{t}_2 decays for $\tan \beta = 2$. As can be seen, for $\mu \leq -400$ GeV the decays into W^\pm, Z^0 dominate, because of the large mass difference $m_{\tilde{t}_2} - m_{\tilde{t}_1}$. In the region $-400 \text{ GeV} < \mu < 1000$ GeV the decays into charginos and neutralinos dominate, the decays into W^\pm, Z^0 being kinematically suppressed because $m_{\tilde{t}_2} - m_{\tilde{t}_1}$ is too small. For $\mu \gtrsim 600$ GeV the branching ratio for $\tilde{t}_2 \rightarrow \tilde{t}_1 A^0$ can go up to 20%. In Fig. 1b we show the branching ratios for \tilde{b}_2 decays as a function of μ and the same set of parameters as above. For $\mu < -600$ GeV the decay $\tilde{b}_2 \rightarrow \tilde{t}_1 W^-$ dominates, and the branching ratio of $\tilde{b}_2 \rightarrow \tilde{t}_1 H^-$ is of the order of 10%. For $\mu > -600$ GeV the decay into neutralinos are the most important ones. The branching ratios for $\tilde{t}_2 \rightarrow \tilde{t}_1 h^0, \tilde{t}_1 H^0, \tilde{b}_1 H^+$ and $\tilde{b}_2 \rightarrow \tilde{b}_1 h^0, \tilde{b}_1 H^0, \tilde{t}_1 H^-$ are always less than 5% for the parameters considered.

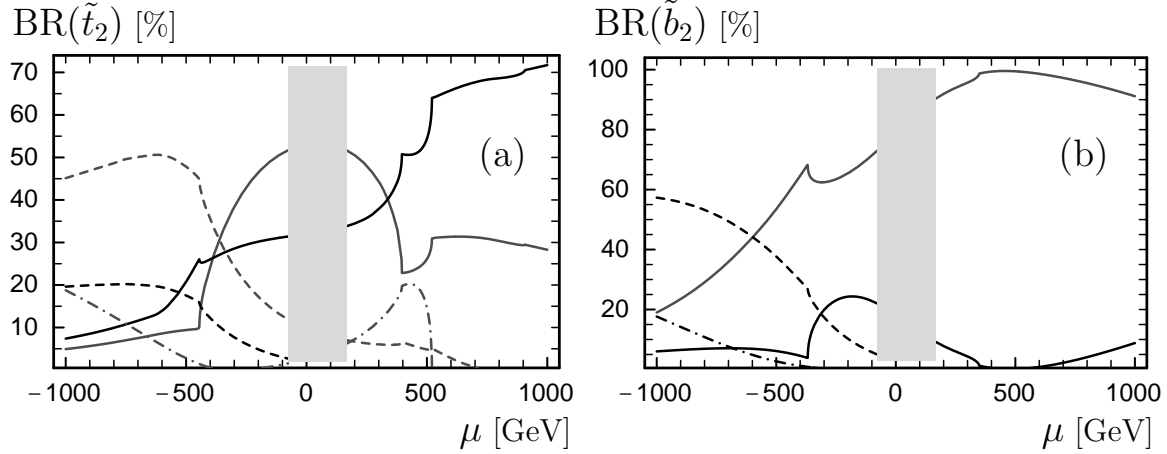


Figure 1: Branching ratios of (a) \tilde{t}_2 decays and (b) \tilde{b}_2 decays, as a function of μ for $\tan \beta = 2$, $M_{\tilde{Q}} = 500$ GeV, $M_{\tilde{U}} = 444$ GeV, $M_{\tilde{D}} = 556$ GeV, $A_t = A_b = 600$ GeV, $M = 200$ GeV, $m_{A^0} = 130$ GeV. The grey areas are excluded by LEP data.

The curves correspond to the following transitions:

- (a) dark full line $\tilde{t}_2 \rightarrow b\tilde{\chi}_i^+$ (summed over $i = 1, 2$), light full line $\tilde{t}_2 \rightarrow t\tilde{\chi}_k^0$ (summed over $k = 1, \dots, 4$), dark dashed line $\tilde{t}_2 \rightarrow \tilde{b}_i W^+$ (summed over $i = 1, 2$), light dashed line $\tilde{t}_2 \rightarrow \tilde{t}_1 Z^0$, dash-dotted line $\tilde{t}_2 \rightarrow \tilde{t}_1 A^0$,
- (b) dark full line $\tilde{b}_2 \rightarrow t\tilde{\chi}_i^-$ (summed over $i = 1, 2$), light full line $\tilde{b}_2 \rightarrow b\tilde{\chi}_k^0$ (summed over $k = 1, \dots, 4$), dashed line $\tilde{b}_2 \rightarrow \tilde{t}_1 W^-$, dash-dotted line $\tilde{b}_2 \rightarrow \tilde{t}_1 H^-$.

Fig. 2a shows the branching ratios of \tilde{t}_2 decays as a function of μ for $\tan \beta = 30$ and the other parameters as in Figs. 1a,b. In this case the decays $\tilde{t}_2 \rightarrow \tilde{t}_1 Z^0, \tilde{t}_1 A^0, \tilde{b}_1 W^+$, and $\tilde{b}_1 \rightarrow \tilde{t}_1 W^+, \tilde{t}_1 H^+$ are allowed in the whole μ range considered. Moreover, the mass differences are $m_{\tilde{t}_2} - m_{\tilde{b}_1} \leq m_{H^+}$ for $-475 \text{ GeV} \leq \mu \leq 546 \text{ GeV}$, $m_{\tilde{b}_2} - m_{\tilde{b}_1} \leq m_Z$ for $-241 \text{ GeV} \leq \mu \leq 281 \text{ GeV}$, $m_{\tilde{b}_2} - m_{\tilde{b}_1} \leq m_{A^0}$ for $-396 \text{ GeV} \leq \mu \leq 436 \text{ GeV}$. The mass of h^0 is in the range $113 \text{ GeV} \leq m_{h^0} \leq 127 \text{ GeV}$. The decays into vector bosons and Higgs bosons, eqs. (10) to (13), dominate for $|\mu| \gtrsim 550 \text{ GeV}$, whereas for $|\mu| \lesssim 550 \text{ GeV}$ the decays into charginos and neutralinos dominate. The branching ratios for $\tilde{t}_2 \rightarrow \tilde{t}_1 h^0, \tilde{t}_1 H^0$ are always less than 5%. Fig. 2b shows the branching ratios of \tilde{b}_2 decays for the same set of parameters. For $|\mu| \gtrsim 400 \text{ GeV}$ the decays into vector bosons and Higgs bosons have the largest branching ratios, whereas for $|\mu| \lesssim 400 \text{ GeV}$ the decays into charginos and neutralinos are the dominant ones. Note that the decay $\tilde{b}_2 \rightarrow b\tilde{g}$ is possible, but its branching ratio is less than 10%. The reason is that it is phase space suppressed. The branching ratios of $\tilde{t}_2 \rightarrow \tilde{t}_1 h^0, \tilde{t}_1 H^0, \tilde{b}_2 \rightarrow \tilde{b}_1 h^0, \tilde{b}_1 H^0$ are less than 5% in the parameter space considered.

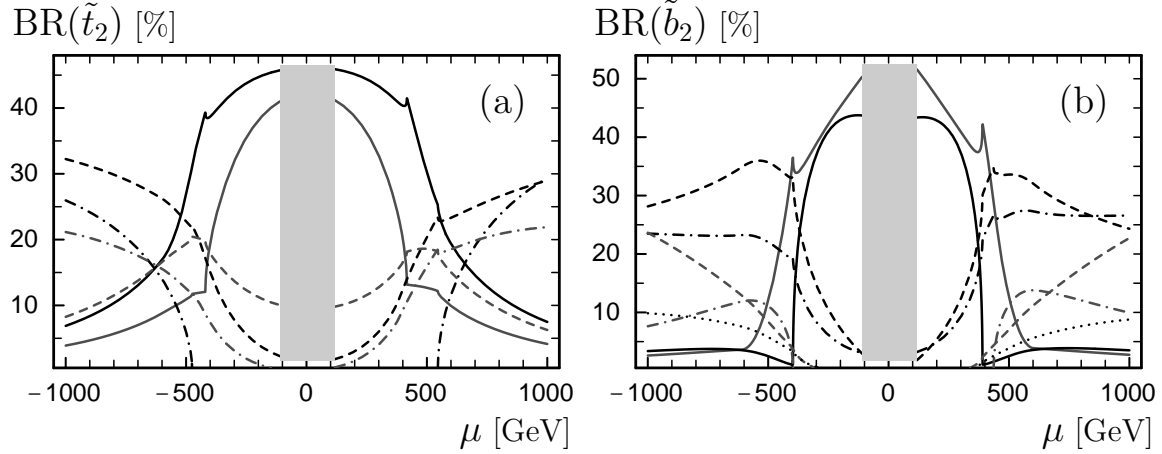


Figure 2: Branching ratios of (a) \tilde{t}_2 decays and (b) \tilde{b}_2 decays, as a function of μ for $\tan \beta = 30$, $M_{\tilde{Q}} = 500$ GeV, $M_{\tilde{U}} = 444$ GeV, $M_{\tilde{D}} = 556$ GeV, $A_t = A_b = 600$ GeV, $M = 200$ GeV, $m_{A^0} = 130$ GeV. The grey areas are excluded by LEP data.

The curves correspond to the following transitions:

- (a) dark full line $\tilde{t}_2 \rightarrow b\tilde{\chi}_i^+$ (summed over $i = 1, 2$), light full line $\tilde{t}_2 \rightarrow t\tilde{\chi}_k^0$ (summed over $k = 1, \dots, 4$), dark dashed line $\tilde{t}_2 \rightarrow \tilde{b}_1 W^+$, light dashed line $\tilde{t}_2 \rightarrow \tilde{t}_1 Z^0$, dark dash-dotted line $\tilde{t}_2 \rightarrow \tilde{b}_1 H^+$, light dash-dotted line $\tilde{t}_2 \rightarrow \tilde{t}_1 A^0$,
- (b) dark full line $\tilde{b}_2 \rightarrow t\tilde{\chi}_i^-$ (summed over $i = 1, 2$), light full line $\tilde{b}_2 \rightarrow b\tilde{\chi}_k^0$ (summed over $k = 1, \dots, 4$), dark dashed line $\tilde{b}_2 \rightarrow \tilde{t}_1 W^-$, light dashed line $\tilde{b}_2 \rightarrow \tilde{b}_1 Z^0$, dark dash-dotted line $\tilde{b}_2 \rightarrow \tilde{t}_1 H^-$, light dash-dotted line $\tilde{b}_2 \rightarrow \tilde{b}_1 A^0$, dotted line $\tilde{b}_2 \rightarrow b\tilde{g}$.

3 Determination of Soft SUSY Breaking Parameters

We perform a case study of $e^+e^- \rightarrow \tilde{t}_1 \bar{\tilde{t}}_1$ at $\sqrt{s} = 500$ GeV, $m_{\tilde{t}_1} = 180$ GeV, and the left-right stop mixing angle $|\cos \theta_{\tilde{t}}| = 0.57$ which corresponds to the minimum of the cross section. The cross sections at tree level for these parameters are $\sigma_L = 48.6$ fb and $\sigma_R = 46.1$ fb for 90% left- and right-polarized e^- beam, respectively. Corrections due to initial state radiation, beamstrahlung, and SUSY-QCD correction have to be applied to the experimental data. Based on our Monte Carlo studies [9], the experimental errors on these cross sections are $\Delta\sigma_L = \pm 6$ fb and $\Delta\sigma_R = \pm 4.9$ fb. Figure 3 shows the resulting error bands and the corresponding error ellipse in the $m_{\tilde{t}_1}$ – $\cos \theta_{\tilde{t}}$ plane. The experimental accuracy for the stop mass and mixing angle is $m_{\tilde{t}_1} = 180 \pm 7$ GeV, $|\cos \theta_{\tilde{t}}| = 0.57 \pm 0.06$.

To treat the sbottom system analogously, we assume that $\tan \beta$ is low and the \tilde{b}_L – \tilde{b}_R mixing can be neglected, $\tilde{b}_1 = \tilde{b}_L$, $\tilde{b}_2 = \tilde{b}_R$, i. e. $\cos \theta_{\tilde{b}} = 1$. Taking $m_{\tilde{b}_1} = 200$ GeV, $m_{\tilde{b}_2} = 220$ GeV, the cross sections and the expected experimen-

tal errors are $\sigma_L(e^+e^- \rightarrow \tilde{b}_1\bar{\tilde{b}}_1) = 61.1 \pm 6.4$ fb, $\sigma_R(e^+e^- \rightarrow \tilde{b}_2\bar{\tilde{b}}_2) = 6 \pm 2.6$ fb for the 90% left- and right-polarized e^- beams.

The resulting experimental errors are $m_{\tilde{b}_1} = 200 \pm 4$ GeV, $m_{\tilde{b}_2} = 220 \pm 10$ GeV. With these results we can predict the mass of the heavier stop, $m_{\tilde{t}_2} = 289 \pm 15$ GeV. This prediction allows experiments to test the MSSM.

Proceeding further we take $\mu = -200$ GeV, $\tan\beta = 2$, $m_t = 175$ GeV, assuming that μ and $\tan\beta$ are known from other experiments. We obtain the soft breaking parameters of the stop and sbottom systems: $m_{\tilde{Q}} = 195 \pm 4$ GeV, $m_{\tilde{U}} = 138 \pm 26$ GeV, $m_{\tilde{D}} = 219 \pm 10$ GeV, $A_t = -236 \pm 38$ GeV if $\cos\theta_{\tilde{t}} > 0$, and $A_t = 36 \pm 38$ GeV if $\cos\theta_{\tilde{t}} < 0$.

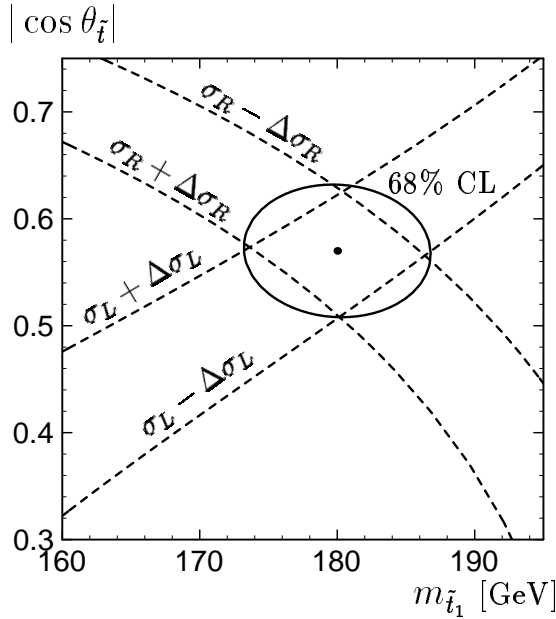


Figure 3: Error bands (dashed) and the corresponding error ellipse as a function of $m_{\tilde{t}_1}$ and $|\cos\theta_{\tilde{t}}|$ for the tree-level cross sections of $e^+e^- \rightarrow \tilde{t}_1\bar{\tilde{t}}_1$ at $\sqrt{s} = 500$ GeV with 90% left- and right-polarized electron beam. The dot corresponds to $m_{\tilde{t}_1} = 180$ GeV and $|\cos\theta_{\tilde{t}}| = 0.57$. The error bands are defined by $(\sigma_L, \Delta\sigma_L) = (48.6, 6)$ fb and $(\sigma_R, \Delta\sigma_R) = (46.1, 4.9)$ fb.

Acknowledgements

We are grateful to K. Hidaka for valuable comments. This work was supported by the "Fonds zur Förderung der wissenschaftlichen Forschung" of Austria, project no. P10843-PHY.

References

- [1] J. Ellis, S. Rudaz, Phys. Lett. B128 (1983) 248.
- [2] J. F. Gunion, H. E. Haber, Nucl. Phys. B272 (1986) 1.

- [3] for a review see, e. g., M. Drees, S. P. Martin, Wisconsin preprint MADPH-95-879, hep-ph/9504324.
- [4] G. Altarelli, R. Rückl, Phys. Lett. B144 (1984) 126;
I. Bigi, S. Rudaz, Phys. Lett. B153 (1985) 335.
- [5] M. Drees, M. M. Nojiri, Nucl. Phys. B 369 (1992) 54.
- [6] A. Bartl, W. Majerotto, W. Porod, Z. Phys. C64 (1994) 499,
erratum Z. Phys. C68 (1995) 518.
- [7] W. Porod, T. Wöhrmann, Phys. Rev. D55 (1997) 2907.
- [8] A. Bartl, H. Eberl, S. Kraml, W. Majerotto, W. Porod, Z. Phys. C73 (1997) 469.
- [9] A. Bartl, H. Eberl, S. Kraml, W. Majerotto, W. Porod, and A. Sopczak, Proc. of the Workshop “ e^+e^- Collisions at TeV Energies: The Physics Potential”, DESY 96-123D, p. 385, ed. P. M. Zerwas;
hep-ph/9701336, to be published in Z. Phys. C.
- [10] A. Arhrib, A. Djouadi, W. Hollik, and C. Jünger, hep-ph/9702426.
- [11] A. Djouadi, J. Kalinowski, P. Ohmann, and P. M. Zerwas, Z. Phys. C74 (1997) 93.
- [12] J. Ellis, G. Ridolfi, F. Zwirner, Phys. Lett. B262 (1991) 477;
V. Barger, M. S. Berger, A. L. Stange, R. J. N. Phillips, Phys. Rev. D45 (1992) 4128.